

Coulomb Stress Change Analysis Center of Celebes on 29th May 2017 6.6 Mw Earthquake and Aftershocks Distribution

Ibrahim¹, Gazali Rachman², and Bagus Jaya Santosa¹

Abstract—Mechanism of earthquakes associated with the distribution of stress static that occurs in rocks. When the rocks elastic limit is exceeded there will be a release of energy as an earthquake result as rocks no longer able to withstand the stress that will disturb the stress field in the neighborhood. In this study, analysis stress of changes was done by taken earthquake data Center of Celebes 6.6 Mw on May 29th, 2017 with hypocenter 13 km using four earthquake recording stations namely BKB, TOLI, PMSI, and LUWI through website GFZ (Geo Forschungs Zentrum) and Global CMT (Global Centroid Moment Tensor), and then calculated the earthquake source parameters so as to obtain model focal mechanism using discretization methods are iterative wave numbers and analyzed using Coulomb 3.3 to obtain the value of Coulomb stress change and its aftershocks distribution. Analysis results showed that orientation the focal mechanism model of earthquake fault plane has been a normal fault type, fault length 27.54 km, width fault 14.06 km with slip shift of 79.06 cm. Coulomb stress Changes are generated ranging from 0.05 to 0.2 bar trending southwest-northwest and northeast-southeast of the epicenter, Based on Coulomb stress plot that center of Celebes 6.6 Mw on May 29, 2017 earthquake triggering aftershocks on May 29th, 2017 at 14:53:44 UTC with latitude and longitude -1.12° and 120.17° northwest trending with a range of values from 0.1 to 0.05 bar, on May 31, 2017 at 04:42:06 with latitude and longitude -1.17° and 120.79° north-east trending with a range of values from 0.15 to 0.1 bar and on November 25, 2017 at 09:14:51 UTC with latitude and longitude -1.18° and 119.93° and 11:11:24 UTC with latitude and longitude -1.19° and 119.94° westbound with a range of values from 0.05 to 0.01 bar.

Keywords—Earthquake, Coulomb Stress, Aftershocks.

I. INTRODUCTION

Celebes is located in a zone of three macro plate enclosures namely the Indian-Australian from the south with an average speed of 7 cm/year, the Pacific plate of the east at a speed of about 6 cm/year and the Asian plate moving relatively passively to the southeast, forming subduction and transform fault. is an active seismic source zone[1]. Figure 1 showing that Earthquake in Celebes is influenced by Palu-Koro active fault that has a depth between 30 to 70 Km. Palu Koro fault extends from north

to southeast and is associated with Matano-Sorong and Lawanoppo-Kendari fault, while at the northern end of Makassar Strait intersected with subduction zone of Celebes Sea Plate. The fault length reaches 500 kilometers starting from the Makassar Strait through the valley of Palu, Kulawi, Koro Valley until it ends in Masamba Sub-district, Luwu District, South Sulawesi. On the Mainland, the length reaches 250 kilometers. The fault is normal and forms a graben. This fault activity has generated many destructive tectonic earthquakes such as the center of Celebes earthquakes May 29, 2017, 6.6 Mw[2]. The Mechanism of a tectonic earthquake is related to the static stress distribution that occurs in the rocks because when the elastic limit of rock is exceeded the fault occurs and the release of energy as an earthquake because the rocks are no longer able to withstand stress. Fractures will encourage stress changes in nearby faults. so it will disturb the stress field in the environment. Increased stress can trigger a fault zone to shift and trigger the occurrence of aftershock. While the stress reduction causes delays in the occurrence of aftershock[3]. The model used to explain the fracture interaction caused by stress is Coulomb stress change.

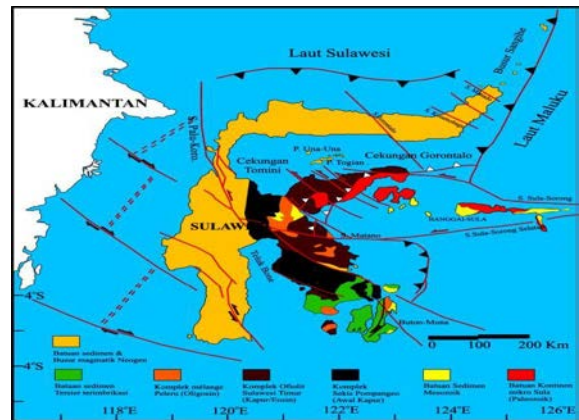


Figure 1. Fault Distribution map of Celebes.

II. METHOD

Analysis of the earthquake of Central Sulawesi May 29, 2017, 6.6 Mw is performed by picking P and S wave data of each recording station to obtain the travel time of the wave through seisgram2k and tauP. The earthquake data was obtained through the official website of the earthquake recorder www.webdc.eu that recorded in three Cartesian components (NS, EW and vertical Z). Figure 2 showing the

¹Ibrahim and Bagus Jaya Santosa are with Physics Department, Institut Teknologi Sepuluh Nopember, Surabaya, 60111, Indonesia. E-mail: baimibrahim094@gmail.com; bjs@physics.its.ac.id.

²Gazali Rachman is with Physics Education Departement, Faculty of Teacher Training and Education, Universitas Pattimura, Indonesia. E-mail: gazali.rachman@gmail.com.

position of six recording stations, namely BKB which is 389.63 km, TOL is 267.20 Km, LUW is 256 Km, PMS 300.60 Km distance, SAN is 623.40 Km and MRS is 244.91 km from the epicenter.

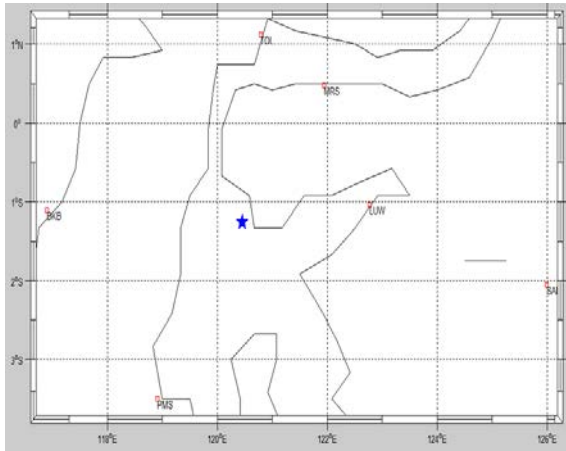


Figure 2. Event and Station Positions

Furthermore, a 1-D velocity modeling using the coupled velocity hypocentre method implemented in vellest 3.3 software was used to obtain a focused and precise wave velocity model for the area research. The data for picking and model of 1D velocity than in inversion using iterative waveform discrimination method through ISOLA GUI software to obtain earthquake source parameters. The subsequent earthquake parameters are used to determine the orientation of the fracture field. Determination of the fault field should be identified because of the ambiguity contained in the source parameter due to the existence of the true fault plane and the auxiliary plane, therefore the HC-Plot method is used to determine the true fault plane[4]. Meanwhile, to determine Coulomb Stress Change after an earthquake and length, the width of the fault field and the length of the slip shift used Coulomb software[5].

III. RESULTS AND DISCUSSION

The wave velocity model is a function of depth (h) to speed. The 1D wave velocity model obtained in this research is as presented in Table 1. The velocity model shows that as depth increases (h) V_p and V_s increase, this is because the deeper, the density of the earth will become denser so the wave velocity will also big. The velocity model obtained is considered to have sufficient precision for the Central Sulawesi region because it has an RMS value of <1 and an average Azimuth 166° GAP where the smaller the RMS value is considered relatively good and will be considered the best if the value of RMS is zero. Which means that if the RMS decodes zero then there is no difference between the results of the observation and calculation, so it is considered that there are almost no differences considered to be considered good. RMS is obtained from the residual difference in travel time between observation time (tobs) and calculation time (tcal) while the good average value of GAP is $<166^\circ$ [6].

TABLE 1.
WAVE VELOCITY MODEL 1D P AND S

Depth (Km)	V_p (Km/s)	V_s (Km/s)
0.0	2.23	1.42
1.0	4.17	2.56
2.0	5.45	3.85
5.0	6.71	3.87
16.0	6.77	3.87
33.0	8.20	4.53
40.0	8.21	4.57
100.0	8.21	4.58
225.0	8.40	4.80

The parameters of the Sulawesi earthquake source mechanism are obtained through the ISOLA-GUI program output. In this research, the filter used to convert data velocity to data displacement in the inversion process is 0.012-0.035 Hz. This filter is used because low-frequency filters for data displacement are useful for meeting the point source approach[7]. Figure 3 showing the four-station displacement observation and synthetic signals with inversion types used in this model, namely deviatoric moment tensor and obtained fitting displacement signal observations of synthetic signals in three-component seismograms with average reduction variance values for all stations 0.84 (84%). Based on the value of variance, the results obtained are said to be good because they have a value of more than 65% and are quite relevant to represent real conditions. Figure 4 showing the fitting of displacement data between observation signals and synthetic signals in three-component seismograms at four reference stations LUW, TOL, PMS and BKB having a normal fault source mechanism with nodal plane 1: strike 102° , dip 30° , rake -94° and nodal plane 2: strike 287° , dip 60° , rake -88° , centroid lat -1.27 , lon 120.45 and depth 13 Km. For more precise results, the source mechanism parameters are then compared with the results of several official earthquake recording sites namely IRIS, GCMT, and BMKG where there are insignificant differences so that the source mechanism parameters can be interpreted to be quite accurate as shown in Table 2.

TABLE 2.
COMPARABILITY OF EARTHQUAKE PARAMETERS MAY 29, 2017, WITH SOME WEBSITE OF EARTHQUAKE RECORDER

Source	Lat	Lon	Depth (Km)	Mag	Strike	Dip	Rake	Beach ball Model
IRIS	1.28°S	120.46°E	12	6.5	101 290	52 38	-94 -83	
GCMT	1.24°S	120.40°E	12	6.6	111 277	34 57	-78 -98	
BMKG	1.27°S	120.45°E	13	6.5	Data Not Available			
Author	1.27°S	120.45°E	13	6.6	102 287	30 60	-94 -88	

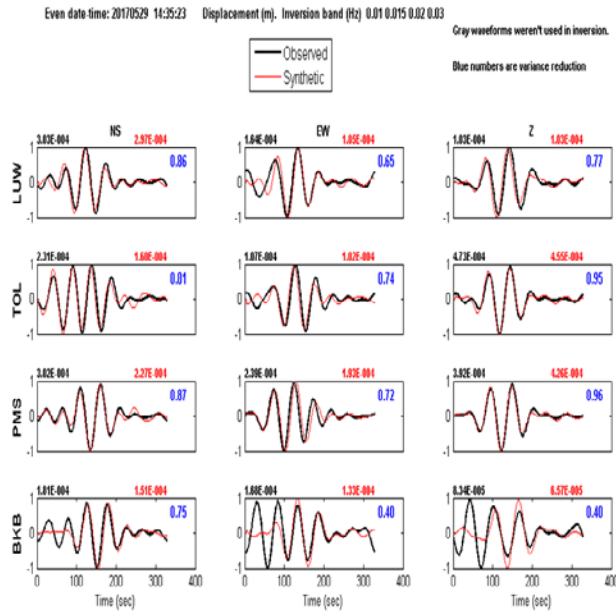


Figure 3. Observation and synthetic displacement signals of four stations

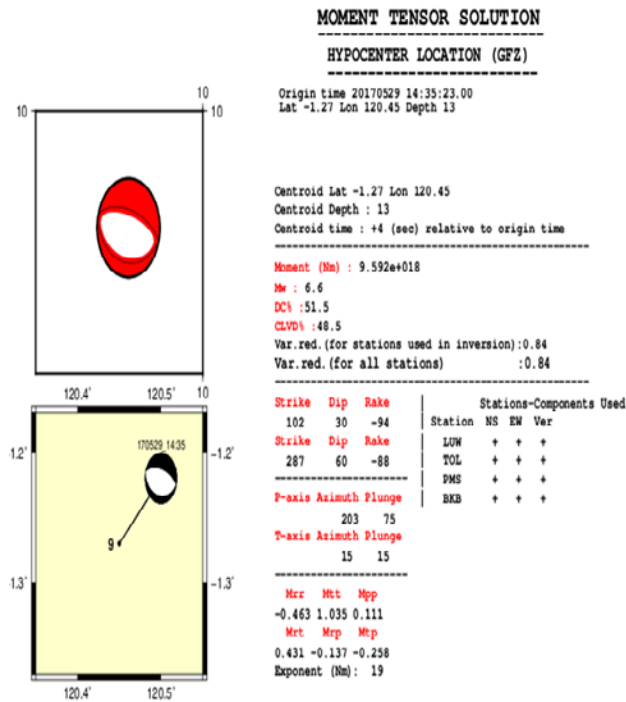


Figure 4. Moment Tensor Solutions

The modeling of the earthquake fracture field of Celebes May 29, 2017, is done using HC-Plot. The principle of the HC-plot method is to test the hypocenter (H) location on both nodes of the plane, when H is located nodal plane 1, the true fault plane is the nodal plane 1 and when H is located in the nodal plane 2, the actual fault is the nodal plane 2 and the other plane is the auxiliary plane. The modeling results show that the actual fault plane orientation is located on plane 2 with strike, dip and rake 287 °, 60 ° and -88 ° located 2.89 km from the hypocenter while the auxiliary plane is located on plane 1 with strike, dip and

rake 102 °, 30 ° and -94 ° located 4.09 km from hypocenter, fault line length 27.54 km, width 14.06 km and large slip shift 79.06 cm as illustrated by figure 5.

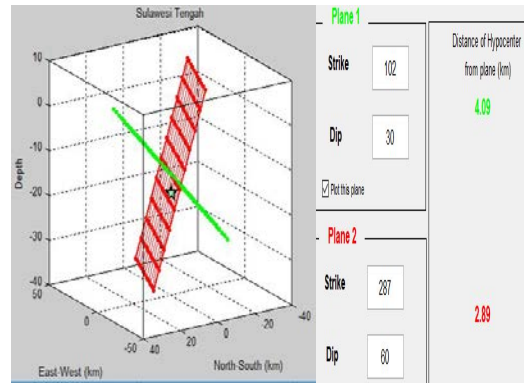


Figure 5. Identification fault fields with HC Plot.

The results of the Coulomb stress analysis are shown in Figure.6 where there are four lobe fields undergoing stress changes consisting of two positive lobe areas or red-yellow stress increases with a stress range of 0.2 to 0.01 bar west and east direction from the epicenter, two negative lobe fields or stress reduction in light blue-blue stress with a stress range of -0.2 to -0.01 bars directed north and south of the epicenter. While Figure. 7. showing the distribution of aftershocks in areas that have increased Coulomb Stress. Distribution of aftershocks caused by an increase in Coulomb stress triggered by the earthquake on May 29, 2017, Mw 6.6 is an earthquake May 29, 2017, with latitude and longitude -1.12 ° and 120.17 ° magnitude 5.02 Mw, depth 10 km, northwest direction with a value of 0.1 to 0.05 bar , 31 May 2017 earthquake with latitude and longitude -1.17 ° and 120.79 °, magnitude 4.96 Mw, depth of 10 km, direction northeast with a range of values 0.15 to 0.1 bar, earthquake 25 November 2017 at 09:14:51 with latitude and longitude -1.18 ° and 119.93 ° and 11:11:24 with latitude and longitude -1.19 ° and 119.94 ° magnitude 5.0 Mw at a depth of 10 km west direction with a range of values of 0.05 to 0.01 bar.

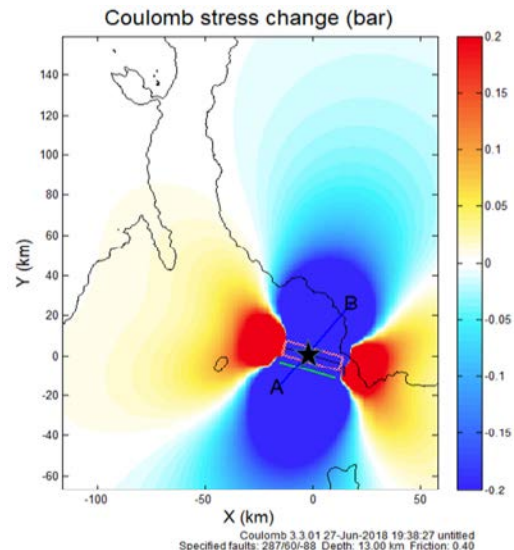


Figure 6. Lobes increase and decrease stress

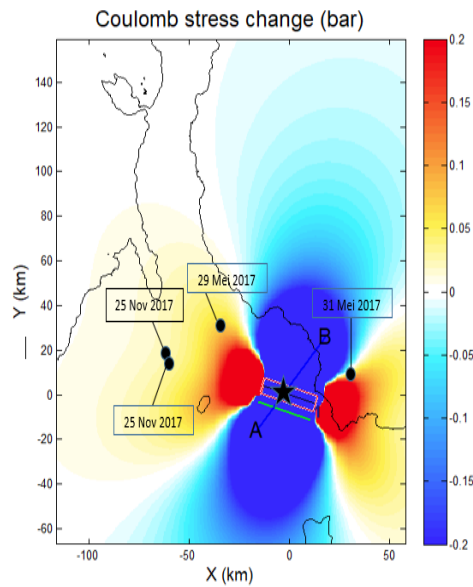


Figure 7. Aftershocks Distribution

Fraction interaction with Coulomb stress changes can be explained by simple coulomb friction model. The potential slip will increase or decrease in Coulomb failure stress, which is defined as:

$$\sigma f = \tau\beta - (\sigma\beta - P) \quad (1)$$

Where σf is Coulomb failure, $\tau\beta$ is shear stress, $\sigma\beta$ is normal stress, P is pore pressure (pore pressure) and μ is the friction coefficient. Potential slip leads to the right or left. The value of σ , in this case, must always be positive, but otherwise, the process in search of the stress value to the fracture can be given positive or negative values depending on the potential slip leading to the right or left[6]. The aftershock of magnitude can be predicted using the following expression:

$$M_w = (1.34 \pm 0.345) \log(L) + (3.8 \pm 0.345) \quad (2)$$

Where M_w is the moment of magnitude, L is the Fault Length (km)[7]. The magnitude of aftershocks occurring around the main quake was obtained in the range of 4.88 M_w - 6.75 M_w as illustrated in Table 3.

TABLE 3.

PARAMETER AFTERSHOCKS DUE TO EARTHQUAKE MAY 29, 2017, 6.6 M_w .

Event	Date	M_w	Lat, Lon	Depth	Region
Aftershock	29 Mei 2017T14:53:44	5.0	-1.12, 120.17	10	Sulawesi, Indonesia
Aftershock	31 Mei 2017T04:42:06	5.0	-1.17, 120.78	10	Sulawesi, Indonesia
Aftershock	25 Nov 2017T09:14:51	5.0	-1.18, 119.93	10	Sulawesi, Indonesia
Aftershock	25 Nov 2017T11:11:24	5.0	-1.19, 119.94	10	Sulawesi, Indonesia
Mainshock	29 Mei 2017T14:35:23	6.6	-1.29, 120.49	13	Sulawesi, Indonesia

IV. CONCLUSION

Model of a focal mechanism of the earthquake of Central Celebes May 29, 2017 M_w 6.6 has normal fault type with length 27.54 km, width 14.06 km, and big slip shift is 79.06 cm. The cesarean orientation has a strike of 287° , dip 60° , rake -88° , centroid lat -1.27 , lon 120.45 and a depth of 13 Km. The stress-increasing area has a range of values from 0.2 to 0.01 bar that flows west and east of the epicenter and the stress drop zone has a range of values of -0.2 to -0.01 bar trending north and south of the epicenter. Increased coulomb stress also increases and decreases the level of seismicity in the surrounding area this is indicated by the presence of Aftershocks distribution in stress-increasing areas. Aftershocks that occurred on May 29, 2017, with latitude-longitude -1.12° 120.17° , May 31, 2017, with latitude-longitude -1.17° 120.79° and dated November 25, 2017 latitude longitude -1.18° 119.93° and latitude-longitude -1.19° 119.94° .

ACKNOWLEDGMENTS

The author would like to thank Prof. Dr. rer.nat. Bagus Jaya Santosa, S.U for his guidance as for the writer doing research. Thanks to Dr. Shinji Toda, Dr. Ross S. Stein, Dr. Volkan Sevilgen and Dr. Jian Lin, on the application guide of Coulomb 3.3 software and thanks to GeoForschungsZentrum (GFZ), IRIS, USGS and Global CMT for seismic and other data surveys.

REFERENCES

- [1] L. Makrup, *Seismic hazard untuk Indonesia*. Yogyakarta: Graha Ilmu, 2013.
- [2] M. S. Kaharuddin, R. Hutagalung, and N. Nurhamdan, "Perkembangan tektonik dan implikasinya terhadap potensi gempa dan tsunami di kawasan Pulau Sulawesi," in *Proceeding The th HAGI and 40th IAGI Annual Convention and Exhibition*, 2011, pp. 26–29.
- [3] Madlazim and J.S. Bagus, "Estimasi Parameter Sumber Gempa Bumi Padang 30 September 2009 , $M_w = 7$, 6 dan Korelasinya dengan Aftershocks-nya," *J. Mat. Sains*, vol. 19, no. 3, pp. 86–91, 2014.
- [4] J. Zahradnik, F. Galovic, E. Sokos, A. Serpetsidaki, and A. Tselentis, "Quick fault-plane identification by a geometrical method: Application to the M_w 6.2 leonidio earthquake, 6 January 2008, Greece," *Seismol. Res. Lett.*, vol. 79, no. 5, pp. 653–662, 2008.
- [5] S. Toda, R. S. Stein, P. A. Reasenber, J. H. Dieterich, and A. Yoshida, "Stress transferred by the 1995 $M_w = 6.9$ Kobe, Japan, shock: Effect on aftershocks and future earthquake probabilities," *J. Geophys. Res. B Solid Earth*, vol. 103, no. 10, pp. 24543–24565, 1998.
- [6] Y. F. Faridiarti, "Relokasi hiposenter dan estimasi struktur model kecepatan 1-D gelombang P di Papua menggunakan velest 3.3," *Inov. Fis. Indones.*, vol. 6, no. 3, pp. 133–139, 2017.
- [7] P. Bormann, M. Baumbach, G. Bock, H. Grosser, G. L. Choy, and J. Boatwright, "Seismic sources and source parameters," in *New Manual of Seismological Observatory Practice (NMSOP)*, Peter Bormann, Ed. Potsdam : Deutsches: GeoForschungsZentrum GFZ, 2009, pp. 1–94.